Title	A TLR9-adjuvanted vaccine formulated into dissolvable microneedle patches or cationic liposomes protects against leishmaniasis after skin or subcutaneous immunization
Authors	Lanza, Juliane S.;Vucen, Sonja;Flynn, Olivia;Donadei, Agnese;Cojean, Sandrine;Loiseau, Philippe M.;Fernandes, Ana Paula S.M.;Frézard, Frédéric;Moore, Anne C.
Publication date	2021-06-21
Original Citation	Lanza, J. S., Vucen, S., Flynn, O., Donadei, A., Cojean, S., Loiseau, P. M., Fernandes, A.P. S.M., Frézard, F., Moore, A. C. (2020) 'A TLR9-adjuvanted vaccine formulated into dissolvable microneedle patches or cationic liposomes protects against leishmaniasis after skin or subcutaneous immunization', International Journal of Pharmaceutics, 586, pp. 1-14. doi: 10.1016/j.ijpharm.2020.119390
Type of publication	Article (peer-reviewed)
Link to publisher's version	10.1016/j.ijpharm.2020.119390
Rights	© 2020, Elsevier B.V. All rights reserved. This manuscript version is made available under the CC BY-NC-ND 4.0 license. - https://creativecommons.org/licenses/by-nc-nd/4.0/
Download date	2024-09-04 11:10:44
Item downloaded from	https://hdl.handle.net/10468/10267

Journal Pre-proofs

A TLR9-adjuvanted vaccine formulated into dissolvable microneedle patches or cationic liposomes protects against leishmaniasis after skin or subcutaneous immunization

Juliane S. Lanza, Sonja Vucen, Olivia Flynn, Agnese Donadei, Sandrine Cojean, Philippe M. Loiseau, Ana Paula S.M. Fernandes, Frédéric Frézard, Anne C. Moore

A TLR9-adjuvanted vaccine formulated into dissolvable microneedle patches or cationic liposomes protects against leishmaniasis after skin or subcutaneous immunization

Juliane S. Lanza[a,b], Sonja Vucen[c], Olivia Flynn[c], Agnese Donadei[c], Sandrine Cojean[b], Philippe M. Loiseau[b], Ana Paula S. M. Fernandes[e], Frédéric Frézard[a] and Anne C. Moore[c,d*]

[a]Departamento de Fisiologia e Biofísica, Instituto de Ciências Biológicas, Universidade Federal de Minas Gerais, Belo Horizonte, Minas Gerais, Brazil;

[b]Antiparasite Chemotherapy, UMR 8076 CNRS BioCIS, Faculté de Pharmacie, Université Paris-Sud, Université Paris-Saclay, Chatenay-Malabry, France

[c]School of Pharmacy and [d]School of Biochemistry and Cell Biology, University College Cork, Cork, Ireland.

[e]Departamento de Análises Clínicas e Toxicológicas, Faculdade de Farmácia, Universidade Federal de Minas Gerais, Belo Horizonte, Minas Gerais, Brazil

*Corresponding author:
School of Biochemistry and Cell Biology, University College Cork, Cork, Ireland. Tel.: +353 21 4205424; fax: +353 214205462. E-mail address: anne.moore@ucc.ie

Abstract

Re-emergence and geographic expansion of leishmaniasis is accelerating efforts to develop a safe and effective *Leshmania* vaccine. Vaccines using *Leishmania* recombinant antigens, such as LiHyp1, which is mostly present in the amastigote parasite form*,* are being developed as a next generation to crude killed parasite-based vaccines. The main objective of this work was to develop a LiHyp1-based vaccine and determine if it can induce protective immunity in BALB/c mice when administered using a dissolvable microneedle (DMN) patch by the skin route. The LiHyp1 antigen was incorporated into cationic liposomes (CL), with or without the TLR9 agonist, CpG. The LiHyp1-liposomal vaccines were characterized with respect to size, protein encapsulation rates and retention of their physical characteristics after incorporation into the DMN patch. DMN mechanical strength and skin penetration ability were tested. A vaccine composed of LiHyp1, CpG and liposomes and subcutaneously injected or a vaccine containing antigen and CpG in DMN patches, without liposomes, induced high antibody responses and significant levels of protection against *L. donovani* parasite infection. This study progresses the development of an efficacious leishmania vaccine by detailing promising vaccine formulations and skin delivery technologies and it addresses protective efficacy of a liposome-based dissolvable microneedle patch vaccine system.

1. Introduction

Leishmaniases, caused by *Leishmania* protozoa, are vector-borne diseases that globally affects up to 2 million people per annum. Visceral leishmaniasis, caused mainly by *L. infantum* or *L. donovani* species, is fatal in up to 95% of cases if left untreated. Current drug regimens suffer from low efficacy, long duration of treatment, toxicity, parasite resistance and cost (Uliana et al., 2018). The fact that individuals who are cured from leishmaniasis develop lifelong immunity against subsequent parasite infections supports the concept of disease prevention through prophylactic vaccination. Advances in understanding the infection pathogenesis and the generation of host-protective immunity, together with the parasite's genome sequencing, has opened new perspectives for vaccine development. However few candidate vaccines have progressed to the clinic (Duarte et al., 2016), there is still a lack of a licensed vaccine to prevent all kinds of human leishmaniasis, similar to many other tropical and neglected infectious diseases (Gillespie et al., 2016). Since the first-generation experimental vaccines against leishmaniasis (i.e. killed whole *Leishmania* parasites) (Noazin et al., 2008) significant advances in this field have been achieved, such as the development of recombinant antigen-based vaccines against canine leishmaniasis (Fernandez Cotrina et al., 2018; Martin et al., 2014; Toepp et al., 2018). *Leishmania* parasites replicate in amastigote form into host macrophages, expressing amastigote-specific proteins to cause and maintain disease. In this context *Leishmania* amastigote-specific antigens are preferred over promastigote ones (Fernandes et al., 2012; Martins et al., 2013). One amastigote-specific antigen that demonstrates promise is LiHyp1 (XP_001468941.1), a 36.6kDa antigen first identified in an extract of axenic *L. infantum* amastigotes by immunoproteomic approaches (Coelho et al., 2012; Duarte et al., 2016; Fernandes et al., 2012). It belongs to the superfamily of 2-oxoglutarate-dependent and iron-dependent oxygenases and its alkylated DNA repair function is considered to be essential for amastigote survival (Coelho et al., 2012; Duarte et al., 2016). Soluble

subunit proteins generally require an immune modulating adjuvant to induce a protective immune response. Among them, liposomes have been widely studied due to their biocompatibility, ability to incorporate a range of compounds and versatility related to size and composition (Li et al., 2019). Due to their characteristic of being easily recognized and taken up by antigen-presenting cells (APCs), liposomes act as a carrier and delivery system for the encapsulated antigen and immunomodulator, resulting in immunoadjuvant action (De Serrano and Burkhart, 2017; Frezard, 1999). Cationic liposomes (CL) have been used as a vaccine platform against infectious diseases`, including those caused by intracellular pathogens. Their key advantages include the high encapsulation efficiency of negatively-charged antigen and immunomodulator and the enhanced uptake by APCs due to strong electrostatic interactions with the cell surface`, associated to induction of specific Th1 and Th17 mediated immune responses 5 (Christensen et al., 2011; Schwendener, 2014). The use of CL adsorbed with unmethylated cytosine-phosphate-guanine oligodeoxynucleotides (CpGs) often shows an improvement in the magnitude of the humoral and Th1-polarized immune response to the co-encapsulated antigen, sometimes shifting the IgG1/IgG2a balance towards a predominant IgG2a response, increasing the antigen-specific release of interferon γ (IFNγ) by CD8+ T cells and favoring protection from *Leishmania* subsequent infection (Bal et al., 2011; Bhowmick et al., 2008; Heravi Shargh et al., 2012).

Currently, vaccines are administrated mostly by parenteral routes, requiring injection of the liquid vaccine. This presents issues with respect to the requirement of needles, syringes and biohazardous sharps waste as well as the requirement for cold chain to prevent vaccine degradation (Kristensen et al., 2016). The skin plays an important and vital role in the pathogen host defense and it contains a high density of dendritic cells. Thus, the skin route of administration has great potential for minimally invasive application of vaccines (Fehres et al., 2013). Microneedle-based delivery systems (MN) consist of micron-sized needles that penetrate skin in a minimally invasive manner allowing application of a broad range of drugs and vaccines (Marshall et al., 2016). One class of MN that has been highlighted for its advantages in vaccine application is the dissolvable microneedles (DMN) (Donadei et al., 2019; Marshall et al., 2016; McGrath et al., 2014; Vrdoljak et al., 2016). These arrays contain the active molecules incorporated into a biodegradable matrix, capable of piercing through the stratum corneum, and then dissolving once placed in the skin, thereby releasing their content. The interest in dissolvable microneedle technology for vaccines has increased in the recent past, mainly due to the development of new, production techniques, which have advantages over some other platforms, such as lack of waste of active material, ease of incorporation of a full dose, enhanced stability of the vaccine and biodegradation of delivery system (Donadei et al., 2019; Marshall et al., 2016; McGrath et al., 2014; Vrdoljak et al., 2016). In addition to safety, an ideal leishmania vaccine should be effective against different *Leishmania* species and should be stable outside of cold chain. Creating a solid dosage form generally results in a more stable vaccine format compared to liquid (Vrdoljak et al., 2016), thereby potentially decreasing vaccine wastage and costs (Duttagupta et al., 2017).

The overall objective of this work was to determine if the amastigote antigen, LiHyp1, induces protective immunity when delivered in a cationic liposome and stabilized and delivered in a DMN patch. We examined the biophysical parameters of a cationic liposome containing the antigen with or without the TLR9 adjuvant CpG. We also characterized physical parameters of the DMN patch containing antigen encapsulated in liposomes and/or formulated with CpG and the effect of DMN incorporation on the liposome. Finally, we determined the immunogenicity and efficacy of vaccines incorporated into DMN patches, compared to a positive control, liquid vaccine, containing both CpG and liposomes, which was injected subcutaneously, in murine model of visceral leishmaniasis caused by *L. donovani*. To our knowledge, this is the first study that examines the protective efficacy of a liposome-based dissolvable microneedle patch vaccine system.

2. Material and Methods

2.1 Materials

1,2-dipalmitoyl-sn-glycero-3-phosphocholine (DPPC, >99%) and 1,2-dioleoyl-3-trimethylammonium-propane (DOTAP, chloride salt, >99%) were purchased from Avanti Polar® (Alabama, US). Bovine serum albumin (BSA), Polycarbonate 0.2µm and 0.1µm-pore membranes, poly(vinyl-alcohol) (PVA), cholesterol (CHOL), chloroform, trehalose, Phosphate Buffered Saline (PBS - pH 7.4), isopropyl-β-D-thiogalactopyranoside (IPTG), Imidazole ACS reagent grade (99%), Urea reagent grade (98%), 4-Chloro-1-naphthol solution, 3,3′-Diaminobenzidine (DAB) and phosphotungstic Acid (PTA) were purchased from Sigma Aldrich (St. Louis, Missouri, USA). Tissue-Plus™ O.C.T Compound, Shandon™ Blue Tissue Marker Dye, NuPAGE® Bis-Tris Precast Gels, Slide-A-Lyzer™ Dialysis Cassettes 7.5K were obtained from Thermo Fisher Scientific Inc. (Massachusetts, USA). 3M® SCOTCH (TM) #810 double-sided tape was used to de-mould the patches. Trichome Masson's stain kit from CellPath (Wales, UK) was used in the histopathology studies. Formvar/carbon coated grids (Cu-300CN; Pacific Grid-Tech, San Francisco, CA) were used in the transmission electron microscopy experiments. Human / mouse CpG-C oligodeoxynucleotide (ODN2395) (Hycult Biotech) was purchased from Cambridge Bioscience (UK) and used as TLR9 immunoadjuvant.

2.2 Expression, purification and physical characterization of recombinant LiHyp1

The plasmid vector pET21aLiHyp1, expressing recombinant LiHyp1 - (XP_001468941.1), a protein member of super-oxygenase family in *Leishmania* amastigotes, was kindly provided by Professor Eduardo Coelho (Sector of Clinical Pathology, Technical College - Coltec, UFMG, Brazil). This plasmid was constructed from the commercial plasmid pET21a (Novagen) with fragment of exogenous DNA obtained from *Leishmania infantum* and related to the gene encoding LiHyp1 (Martins et al., 2013). The plasmid vector was transformed into *Escherichia coli* (C41 strain), colonies were checked for cloning confirmation, selected, expanded in LB culture media supplemented with Ampicillin 100 µg/mL and, stimulated with 1mM of expression inducer IPTG for 3 hrs at 37°C, 180rpm stirring. The bacteria were pelleted, lysed in PBS containing 8M urea and 40mM imidazole and treated for purification by nickel affinity chromatography HisTrap™ HP coupled to FPLC (GE Healthcare Life Sciences) as previously described (Martins et al., 2013). The purified His-tag rLiHyp1 protein solution was dialyzed in PBS 4M urea, treated for LPS elimination (EndoTrap® red Endotoxin Removal Kit) according to manufacturer's

4

specification, and quantified using the Lowry method, modified by Peterson (Peterson, 1977) and confirmed by absorption spectrometry at 280 nm. This antigen preparation was used for liposome preparation or aliquoted and freeze-dried. The procedure is schematized in **Fig. 1A.** Western Blot using anti-His monoclonal antibody (GE Healthcare life Sciences, diluted 1:3000 in blocking buffer) was used to confirm rLiHyp1 constitutive expression and purity . Antibody binding was detected with peroxidase-coupled anti-mouse IgG (HRP) (Millipore, Temecula, California, USA, diluted 1:5000). After further washing, the recombinant antigen (rAg) was revealed by the reaction of Chloronaphthol and DAB with 30% H_2O_2.

2.3 Preparation and characterization of cationic liposome (CL) formulations of antigen
Cationic liposomes (CL) were made from lipids DPPC, CHOL and DOTAP at 6:2.4:3 molar ratio. Antigen was encapsulated in liposomes using a dehydration–rehydration technique (Zadi and Gregoriadis, 2000). Briefly, a suspension of liposomes was first obtained at 50 g/L lipid, through hydration of the lipid film with deionized water, submission to freeze and thaw cycles and then repeated extrusions (5 cycles) across 0.2 μm and 0.1 μm pore polycarbonate membranes (Nayar et al., 1989). The resulting empty unilamellar liposomes suspension was then mixed with the compounds to be encapsulated (bovine serum albumin, BSA or LiHyp1 protein at 20 g per mole of lipid; CpG ODN at 1.8 g per g of protein). Trehalose was added as cryoprotectant (at 3:1 sugar/lipid mass ratio and the mixture was immediately lyophilized (freeze-dryer L101; Liotop, São Carlos/SP, Brazil). and stored at -20°C until use. For liposome reconstitution, ultrapure water was added to freeze-dried samples at a final trehalose concentration of 15% (w/v) and suspensions were incubated for 30 min at 45°C with intermittent vortexing. The liposome formulations intended for subcutaneous immunization were diluted at 100 μg/mL of protein with PBS and then submitted to dialysis (7.5K – Slide-A-Lyzer™ Dialysis Cassettes) against PBS containing 0.8M urea. Liposome samples intended for incorporation into DMN patches were dialyzed against a solution of trehalose 15% (w/v) and PVA 1.25% (w/v) containing 0.8 M urea. The particle size distribution and zeta-potential were first evaluated by dynamic light scattering (DLS) , using a Malvern's Zetasizer Nano ZS instrument (Malvern Instruments, Worcestershire, UK) with the detector at 173° angle and 100.000 counts/s. Electrophoretic mobility of samples was converted in Zeta potential (ζ, mV) by Malvern Panalytical Software v3.30 using Smoluchowski equation. In the case of polydisperse samples with polydispersity index (PDI) higher than 0.3, particle size was further assessed by Nanoparticle Tracking Analysis, (NTA®) version 3.0 0064 (NANOSIGHT, Malvern Instruments, UK) (Filipe et al., 2010). For the analysis, NTA 3.2 Dev Build 3.2.16 program was used, with the following image capture configurations: 5 threshold, 15 Gain, Automatic Luminosity and Blur. Measurements were carried out at 25°C and at the day of liposomes resuspension and repeated at least three times for each sample. Protein encapsulation efficiency into liposomes was determined by quantification of free and encapsulated protein, in PBS reconstituted DMN or liquid samples, using the Lowry method (Peterson, 1977). LiHyp1-liposomes were separated from free protein by centrifugation at 20,000 x g for 15 min at 4°C. and washing 3 times with PBS. Protein content in all washes was determined. Protein encapsulation rate was determined according to the following formula:

$$Encapsulation\ rate\ (\%) = \frac{Amount\ (\mu g)\ of\ entrapped\ protein}{total\ amount\ (\mu g)\ of\ protein\ in\ the\ formulation}$$

2.4 Liposome-containing DMN patches

2.4.1 Production of liposome-containing dissolvable microneedle patches.

DMN patches contained 25 microneedles in a 1-cm^2 area (**Fig. 2B**). Each microneedle was 500 μm in height and had a 3:2 height : base ratio (O'Mahony, 2014). Patches were prepared as previously described (Vrdoljak et al., 2016). Briefly, formulation was delivered directly onto water-filled microneedle cavities in a polydimethylsiloxane (PDMS) mould at a rate of 8 µl/min. Formulation in the moulds was dried overnight at 25°C and 10 mBar of pressure and then pulled from the mould onto medical grade adhesive tape (1525 L-Poly-Med tape, 3 M) (Donadei et al., 2019; Vrdoljak et al., 2016).

2.4.2 Characterization of antigen and liposomes in DMN patches

Lack of degradation of rLiHyp1 in DMN patches was determined by dissolving patches in PBS and assessing its migration by 12% SDS-PAGE, using NuPAGE® Bis-Tris Precast Gels (Thermo Fisher Scientific Inc., Massachussetts, USA) according with the manufacturer protocols. To assess the morphology and size integrity of the liposomes after incorporation into DMN, patches were completely dissolved into 1 mL of PBS and samples were submitted to Electron Transmission Microscopy and NTA. Samples were applied onto the formvar/carbon coated grids by drop to drop method and subsequently negative stained with PTA at 1%. Ten μl of liposomes (dilution 50X) in PBS were dropped onto the grid and allowed to adsorb for around 1 min. The surplus was removed by filter paper (Whatman #44) and the grids were washed three times in deionized water droplets and then, immersed in a staining (PTA 1%) droplet, blot in a filter paper, and let air dry overnight. Samples were analyzed using a Jeol 2000FXII Transmission Electron Microscope (TEM) operating at an acceleration voltage of 80KV, line resolution of 0.34 nm, point resolution of 0.49nm, and Cs of 6.3 (spherical aberration), implying high contrast (model Tecnai G2 Spirit, 2006; FEI). Representative electron micrographs were taken at magnifications of X80.000 to X200.000. The particles size was assessed by TEM and compared with the results obtained by NTA. Based on the 8-µL volume of formulation per patch, the amount of protein per patch could be estimated as 5 µg.

2.4.3 Visual assessment and Score of DMN patches

DMN were visually evaluated using an Olympus BX51 optical microscope. DMN images were recorded with an Olympus DP70 digital camera (Olympus, USA), coupled above objective microscope lenses with 400X magnification. A scoring system was used to grade the physical quality of 1 cm^2 patch units; a patch with a score of 100 reflected a patch where all 25 microneedles per 1cm^2 were perfectly formed (**Table 1**). A value of 88 was given for the lower level of specification (LSL) based on historical qualitative results (>22 perfect MN per patch consisting of perfect 8-sided DMN) (**Table 1**). In order to closely analyze the DMN texture, their surface was imaged by scanning electron microscopy (SEM), using a JEOL JSM 5800 (JEOL USA Inc, Peabody, MA, USA) at 3 kV microscope equipped with an ISIS EDS 300 analyzer. Samples without any treatment were fixed with a double-sided adhesive tape in a metal support and subjected to vacuum for analysis.

2.4.4 *Mechanical Properties of Liposome DMN patches*

Mechanical properties of the microneedles, specifically the pressure required to cause compression or breakage of the DMN, were assessed using a TA.XT-plus Texture Analyser (Stable Micro Systems, Surrey, UK) by application of a known axial compression load to DMN structures. DMN patches were attached to a cylindrical probe (length 3.5 cm, cross-sectional area 1.5 cm^2) using double-sided adhesive tape (3M) and pressed against a flat block of aluminum of dimensions 9.2×5.2 cm at a rate 0.5 mm/s until complete compression. Pre-test and post-test speeds were 1mm/s while the trigger force was set at 0.049 N. Test conditions included application of an increasing axial load until a probe displacement of 0.5 mm occurred or application of known force with measurement of probe displacement. Three samples from each batch (score ≥92) were evaluated. Measurements were carried at room temperature and humidity. The results are expressed as the maximum pressure (force, per unit of cross section area) (N/m^2) that the DMN material withstood before it compressed. Sudden breakage of microneedles was not observed.

2.5 Skin insertion studies

Porcine skin was used as a model for *in vitro* DMN skin penetration studies, as previously described (McGrath et al., 2014; Vrdoljak et al., 2016). Twenty-four hours before use, frozen porcine ears were thawed at 4°C, shaved and subcutaneous fat was removed with a scalpel. Microneedle patches were pressed for 3 sec, perpendicularly to the skin with a handmade, spring-loaded applicator, calibrated for 10N. Patches were then withdrawn immediately from the skin or left in place for 1, 3, 5, 15, 30 and 60 min after insertion in the skin, in the same manner as previously reported (Paleco et al., 2014; Vucen et al., 2013). Microneedles were assessed by microscopy before and after the applications in order to evaluate the needles dissolution kinetics. In all studies, the skin was subsequently stained with Shandon^{TM} Blue Tissue Marker Dye (Thermo Fisher Scientific, USA) for 5 minutes. Excess dye was then removed with a swab wetted with PBS. The DMN-applied skin was excised and snap-frozen in O.C.T. medium. The frozen skin samples were cryo-sectioned into 10μm transverse sections, analyzed in bright field microscopy and subsequently stained with Trichome Masson's stain.

2.6 Immunogenicity and efficacy of LiHyp1 vaccines

2.6.1 Animals and parasites

Female BALB/c mice, 4-6 weeks old (Envigo, UK) were used in the experiments for evaluation of the humoral and cellular immune response (n = 5 mice per group). These experiments were carried out in accordance with the European Directive 2010/63/EU, and under an authorization issued by the Health Products Regulatory Authority Ireland (license number AE19130/P030) and approved by the Animal Ethics Committee of University College Cork. For efficacy studies, female BALB/c mice (Élevages Janvier, Le Genest Saint Isle, France) aged 6-8 weeks and 18-20 g body weight were used (n ≥ 7 mice per batch). Vaccine efficacy studies were approved by the Committee Institutional Ethics for the Handling of Animals at the Université Paris-Sud (CEEA 26-063/2013). *Leishmania donovani* amastigotes (MHOM/ET/67/HU3 - also designated LV9) were obtained shortly after spleen isolation from previously infected *Mesocricetus auratus* (Golden Hamsters). Spleens were macerated in M199 culture medium (Gibco®, Invitrogen, NY, USA), pH 7.0 supplemented with 0.1 mM adenosine, 5 μg/mL

7

hemin, 25 mM HEPES, 50 µg/mL penicillin and streptomycin (Sigma-Aldrich, St Louis, USA) 1%(v/v) inactivated FBS (Gibco®, Invitrogen, NY, USA). The tissue homogenate was submitted to a series of centrifugations and lysis to release the amastigote from the infected cells, that were subsequently counted and adjusted to the concentration of 10^7 amastigotes/mL (Balaraman et al., 2015).

2.6.2 Immunization protocol

BALB/c mice were immunized three times with 14-days intervals (days 0, 14, 28). Doses of each component were kept constant across all groups, i.e., 10 µg LiHyp1, 18 µg CpG and 250 µg lipids. For DMN patch administration, each patch consisted of 5 µg LiHyp1, 9 µg CpG and 125 µg lipids; 2 patches were administered to each animal. Five LiHyp1 vaccine groups were tested (n = 5 per group): (a) CL+CpG:SC; representing a control group consisting of the liquid LiHyp1 plus CpG liposomal formulation applied subcutaneously (SC) in 100 µL, (b) CL+CpG:DMN; LiHyp1 plus CpG in cationic liposomes in DMN, (c) CL:DMN; LiHyp1 in cationic liposomes in DMN (no CpG), (d) CpG:DMN; a non-liposomal formulation of LiHyp1+CpG in DMN (no liposomes) and; (e) 100 µL of PBS injected subcutaneously. For each patch administration, the mice were pre-anesthetized with isoflurane and the patches were applied to the dorsal surface of each ear, pressing the fingers against the animals' skin for 10 sec, and left in place overnight.

2.6.3 Immunogenicity evaluation

Mice were euthanized twelve days after the third immunization (day 40). Serum samples were stored at -20° C and spleens were homogenized and cryostored until use. Antibody responses to LiHyp1 were evaluated by ELISA, as previously described (Joyce et al., 2018). Briefly, microtiter plates (MaxiSorp: Nunc) were coated with 2 µg/mL recombinant LiHyp1 in 1X carbonate buffer (0.1 M at pH 9.6). Plates were incubated overnight at 4°C, then washed with PBS + 0.05% Tween 20 (PBST) and blocked with 1% Bovine Serum Albumin (BSA) for 1 hr. Serum samples were serially diluted in 1% BSA solution and added to the coated plate. After a 2-hr incubation, washed plates were incubated with goat anti-mouse IgG-HRP (1/10,000) or alternatively, anti IgG1-biotin or IgG2a-biotin. After a 1-hr incubation antigen-specific antibodies were detected with 3,3',5,5'-tetramethyl-Benzidine (TMB) substrate (BioLegend). Plates were then read at 655nm and titers were determined using endpoint titer method. Endpoint titers were taken as the x-axis intercept of the dilution curve at an absorbance value 3x standard deviations greater than the absorbance for naïve mouse serum. For analysis of antigen-specific Th1/Th2 induction, splenocytes were thawed and stimulated at 2×10^6 cells/ml in a total of 200 µL in 96-well culture plates (Costar, Corning, NY, USA) with LiHyp1 (1 µg/well) or Concanavalin A (ConA; 1 µg/well). Plates were incubated at 37°C, 5% CO_2 for 48 h when culture supernatants were collected. Cytokine sandwich ELISA was performed to evaluate the production of IFN-γ and IL-10 using the reagents and specifications of the BD Kits OptEIA Mouse IFN-γ or IL-10 ELISA Set (BD, San Diego, CA, USA).

2.6.4 Vaccine efficacy

Twenty one days after the last immunization, BALB/c mice were challenged with infection of *Leishmania donovani* parasites with an inoculum of 1×10^6 amastigotes per mouse, intravenously by the ocular orbital plexus. Fifteen days after infection, animals were sacrificed, and the spleen and liver were individually collected. The organs were macerated in PBS in a 1:10 w/v and 200 µL from each

homogenate was added to lysis buffer plus proteinase K and incubated at 56°C overnight for complete tissue lysis. Genomic DNA (gDNA) was extracted from the samples with the illustra tissue and cells genomicPrep Mini Spin Kit' (GE Healthcare®), following the manufacturer's instructions and quantified by spectrophotometry using Tecan NanoQuant plate in Spark® Multimode Microplate Reader (Tecan, SWI). Real Time PCR (qPCR) was performed with a total amount of 50ng of gDNA of each sample, for quantification of *Leishmania* gDNA and determination of the parasite load in the organs and efficacy of vaccine protection. Primers used were: forward 5'-CCTATTTTACACCAACCCCCAGT-3 '[JW11], and reverse 5'-GGGTAGGGGCGTTC TGCGAAA-3' [JW12]), constructed for the amplification of a 120 bp specific region of minicircle present in *Leishmania sp.* kinetoplast DNA (kDNA) (Nicolas et al., 2002; Santi et al., 2018). gDNA from a known number of *Leishmania donovani* promastigotes was also extracted, dosed and serially diluted for construction of a standard curve from 5000 to 0.05 pg, corresponding to 500 to 0.5 parasites, according with the correlation: 1 leishmania parasite = 1 entire genomic DNA = 0.1 pg of gDNA weight (Manna et al., 2008; Marfurt et al., 2003). The determination of parasites of each normalized sample was made by interpolation of gDNA amplification Ct interpolated in linear regression graph of amplification Ct vs. leishmania gDNA weight in pg of the standard curve (Santi et al., 2018).

2.7 Statistical analysis

Statistical analyses were performed in GraphPad Prism® 5.0 software using the Kruskal Wallis non-parametric test and Dunns (or Mann Whitney) test for non-normal distribution data, and the one-way ANOVA with Bonferroni post-test (or Test t) for normal distribution data.

3 Results

3.6 Characterization of purified LiHyp1

In this work, the *Leishmania infantum* amastigote-specific protein LiHyp1 (XP_0014689 41.1) was expressed in *Escherichia coli* (C41 strain) and the recombinant antigen, fused with an N-terminal 6x histidine tag, was purified by FPLC (**Fig. 1**) and included in the vaccine formulations.

Urea was present at high concentration (8 M) in rLiHyp1 purification buffer to promote protein solubilization, as rLiHyp1 is mostly present in insoluble bacteria extract (Coelho et al., 2012; Martins et al., 2013). We first determined the effect of urea concentration on antigen aggregation using DLS and confirmed by NTA, after dialysis into PBS or the DMN matrix formulation (trehalose 15% w/v + PVA 1.25% w/v). It was observed rLiHyp1 forms aggregates in PBS at 8 M urea with average hydrodynamic diameter of 70.0 ± 8.3 nm (PDI = 0.20 ± 0.02) (**Table 2**). Reduction of urea concentration to 4 M resulted in increased particle mean diameter and polydispersity (diameter of 198.5 ± 7.6 nm with PDI = 0.37 ± 0.01), suggesting an increase of rLiHyp1 aggregation (**Table 2**). Dialysis of rLiHyP1 in PBS at urea concentrations lower than 4 M caused rLiHyp1 precipitation in the dialysis cassette, suggesting super-aggregation. Dialysis of rLiHyp1 samples in DMN matrix formulation containing 0.8 M urea did not result in further protein aggregation or precipitation, as evidenced by the resulting homogenous colloidal solution with low PDI (0.17±0.02) and intermediate size, around 158.4±9.7(**Table 2**).

2.6 Preparation and characterization of antigen in cationic liposomes (CL) and in DMN patches

The encapsulation of the antigenic protein in CL was performed according to the dehydration-rehydration method (Zadi and Gregoriadis, 2000). We chose this process because it has been shown to preserve protein structure and allow high encapsulation rate. The use of trehalose as excipient has a double function: to control membrane fusion during the freeze-drying process and the final liposome size; to generate a matrix compatible with posterior incorporation into DMN that also contain trehalose as main component. Formulations of rLiHyp1 free (+ CpG) and rLiHyp1 liposomal (+ or - CpG) were prepared, dialyzed against DMN matrix at 0.8M urea and used to produce DMN patches. The macroscopic and biophysical features of the different rLiHyp1 formulations before and after the DMN manufacturing process are described in **Table 2** and **Fig. 2 .**

To characterize the antigen-liposome formulation, firstly the rLiHyP1 encapsulation rate (ER) was assessed. Approximately 41% of rLiHyp1 added to CL remained associated to liposomes, while the addition of CpG to the formulation increased protein encapsulation up to 75% (**Table 2**). When rLiHyp1 in liposomes (+/- CpG) were recovered from DMN, a reduced amount of antigen was found to be encapsulated compared to the starting material (**Table 2**; liposome encapsulated versus solid).

Secondly, the particle size and morphology of the rLiHyp1 formulations were determined. Due to the high polydispersity index (PDI>0.5) of liposomal samples, measured by DLS, the particle diameter was determined by NTA. Liposome-encapsulated rLiHyp1 showed an average diameter around 200 nm and a positive zeta potential, with no significant change in these characteristics in the presence of CpG or after incorporation/dissolution of DMN (**Table 2**). One concern of formulating antigen-based liposomes into DMN patches was the integrity of the liposomes after dissolution of DMN. DLS, NTA size measurements and TEM images confirm that the vesicles could be recovered after DMN resuspension with similar size (~100-200nm) (**Fig. 3**). However, it is noteworthy that a higher polydispersity was observed in the liposome formulations after DMN incorporation and dissolution compared to the liquid formulation. In addition, TEM images of smaller, high contrasted aggregates outside or attached to the vesicle's membrane, might represent rLiHyp1 aggregates, observed to be more numerous in the case of solution recovered from DMN. This may represent a concentration of rLiHyp1 aggregates outside of the vesicles, consistent with the significant reduction in the ER observed after insertion of liposomes into the DMN. Production of DMN patches was then assessed. The presence of urea (4M) in the CL, CpG and antigen formulation resulted in unacceptable microneedle formation, when BCG was used as antigen (**Supplementary Table 1, Supplementary Figure 1**). Thus urea was removed from all subsequent DMN formulations. The physical characteristics of the rLiHyp-1 microneedle patches were assessed. The DMN scores for all patches containing the 3 different rLiHyp-1 formulations were excellent (**Table 2**). The mechanical robustness of rLiHyp1 liposomal DMN were approximately 10N. (**Table 2**). Omission of the CL produced a DMN with substantially higher mechanical strength, an average pressure of 17.4 N/m^2 was required to be applied before DMN compressed, compared to DMN that incorporated CL. This indicates that inclusion of cationic liposomes weakens the DMN patch.

Overall, these results demonstrated that the conditions to produce a liposomal LiHyp1 formulation incorporated into DMN produced patches of adequate physical characteristics of the microneedle and known physical stability of the liposomes in DMN.

2.7 Skin penetration studies

We next sought to determine the capacity of DMN patches to penetrate skin. In this study, BSA was used in DMN patches as a surrogate antigen. DMN patches with soluble antigen or antigen incorporated into CL (+ or – CpG) were assessed for skin penetration and dissolution. After manufacture, 5 patches per batch of each DMN type, i.e., BSA in CpG:DMN, CL:DMN or CL+CpG:DMN , were examined for their ability to pierce cadaver porcine skin. A kinetic study of the DMN dissolution after application and removal from skin was performed to determine the minimum contact time for the patches that allowed a complete dissolution of DMN in the dermis. The insertion of the patches into the skin requires an estimated force of 10 N (McGrath et al., 2014). To ensure a 10 N force, a manual applicator with a force of 10 N was used to press the DMN patches into the skin for 3 seconds. After this application patches were removed immediately or after 1, 5, 15, 30 and 60 minutes of contact with the skin, and analyzed by optical microscopy (**Fig. 4**).

All batches of DMN patches had similar dissolution kinetics and skin perforation pattern with no differences detected across the groups (*data not shown*). After 15 minutes of administration in the skin, microneedles were completely dissolved; no further dissolution or penetration occurred after this time (**Fig. 4**). To demonstrate skin perforation after DMN application, the site of administration was stained with methylene blue (**Fig. 5B**). Skin indentations were distinguished by the regular blue dots where the microneedles on the patch had penetrated the skin. Skin ruptures were observed (**Fig. 5C and D**). Stained images demonstrated that disruption made by the DMN go into the dermis, where there is a presence of collagen (stained in blue) (**Fig. 5D**).

2.8 Immunogenicity of vaccines in mice

The primary objective of the *in vivo* studies was to identify which vaccine in a DMN patch induced the highest protective immune response. The cellular and humoral immunogenicity of LiHyp1 in DMN patches, free or incorporated into liposomes, with or without CpG was evaluated and compared to a control vaccine regime of subcutaneous injection with liquid vaccine composed of rLiHyp1 incorporated into CL and with CpG. Immunization with LiHyp1 and CpG and CL by the SC route, termed CL+CpG:SC, induced high IgG antibody titres (**Fig. 6A**), which were dominated by an IgG1 isotype (**Fig. 6B, C, D**). Immunization with rLiHyp1 + CpG, without liposomes, using DMN patches onto the skin (CpG:DMN) induced a total IgG response that was equivalent to the positive control vaccine given by the SC route. The antigen-specific IgG1 and IgG2a titers were not significantly different between the CpG:DMN and the liposome-based vaccine injected SC. Delivery of liposome-based vaccines using DMN into the skin, with or without CpG, termed CL+CpG:DMN and CL:DMN respectively, induced significantly lower IgG responses compared to the injected vaccine. Furthermore, low titers of IgG1 and IgG2a were observed in some mice immunized with these liposome-based DMN; these antibodies were undetectable in other mice in these groups (Fig 6B, C). Despite these low titers, there is a trend that the

11

addition of CpG to the liposome can skew the phenotype of the antibody isotype towards a stronger IgG2a response (**Fig. 6D**). However, addition of CpG had no effect on increasing the magnitude of the antibody response. These findings demonstrate that although the liposome-based vaccine is immunogenic when injected, its potency is significantly decreased when delivered by a DMN patch. However, the antigen, adjuvanted with CpG, is as immunogenic as an injected liposome vaccine when administered into the skin with a DMN patch.

The Th1/Th2 phenotype of the response was also assessed in thawed spleen cell populations. The potential of thawed spleen cells to produce cytokines was assessed by responses to the mitogen, ConA. It can be seen that the cytokine-producing capacity of spleens from mice injected with the CL+CpG:SC and the CL+CpG:DMN were very low, suggesting that T cells were generally non-viable (**Fig. 7**). In contrast, spleens from the other two vaccinated groups responded well to ConA by producing IFN-γ and low levels of IL-10. It can be seen from these two responding groups (CL+CpG:DMN and CL:DMN) that addition of CpG to the liposome and administration using a DMN patch can increase the production of antigen-specific IFN-γ compared to skin administration of the antigen-encapsulated liposome alone, in some mice. Overall, little IL-10 was observed above the background level observed when spleen cells from naïve mice were stimulated with antigen.

2.9 Protective efficacy of skin vaccination in mice

Vaccine efficacy was assessed by challenging immunized mice and naïve controls with *Leishmania donovani* amastigotes three weeks after the final immunization, Parasite load was assessed in liver and spleen. Significant protection against liver infection was induced in animals that were immunized with liposomes by the subcutaneous route (CL+CpG:SC) and when the antigen and CpG were administered into the skin using a DMN patch (CpG:DMN) (**Fig. 8**). Significantly decreased parasite load was also observed in the spleen but not in the liver when the antigen was encapsulated in liposomes, without CpG and delivered with a DMN patch (CL:DMN). Partial protection (50% parasite suppression in the liver and >90% in the spleen) due to the skin vaccination with the LiHyp1:CL:DMN formulation was observed. dno significant protection in either organ was induced by skin vaccination with the LiHyp1+CpG:CL:DMN vaccine. Thus, while the subcutaneous LiHyp1:CL+CpG vaccine confers an overall parasite suppression of 70%, the skin-based LiHyp1+CpG:DMN vaccine was the most effective one, with a protection rate > 90% in the two analyzed organs (**Fig. 6**).

3 Discussion

Much has been done towards the development of a vaccine to prevent human leishmaniasis. Nevertheless, despite some first-generation formulations advancing to clinical trials, there is still no evidence of effective human protection against *Leishmania* infection (Gillespie et al., 2016), whereas some vaccines are already licensed for canine leishmaniasis. A human vaccine requires appropriate antigen and adjuvant delivery system and route of administration, so as to achieve high protection efficacy, safety, stability under storage and transport as well as low cost of production. Skin-based

vaccination systems containing second-generation antigen, nanoparticles and dissolvable microneedle patches, could provide efficient strategies to circumvent these problems. In the present work we designed an adjuvant system for rLiHyp1, a *Leishmania* amastigote-specific oxygenase recombinant protein, obtained by heterologous expression and purified in reasonable yield, based on cationic liposomes, with or without CpG and in dissolvable microneedles or by injection. We demonstrate that vaccination with a DMN patch incorporating the TLR9-adjuvanted antigen induced a high level of protective immunity mice against *L. donovani* infection. Our results indicate that this skin patch vaccine is as immunogenic and efficacious as an injected vaccine. In contrast, the immune response and efficacy was found to be eliminated when cationic liposomes were incorporated in the patch. To the best of our knowledge, this is the first report of induction of protective efficacy in experimental visceral leishmaniasis using a recombinant antigen-based dissolvable microneedle patch strategy.

Immunoproteomic studies identified several immunogenic proteins in *Leishmania infantum* amastigote and promastigote extract, as well as their binding affinity to specific CD8+ and CD4+ T-cell epitopes, in order to obtain purified recombinant antigens to test as immunodiagnostics and vaccine candidates against leishmaniasis (Coelho et al., 2012; Duarte et al., 2016). Some of them, like LiHyp1, showed high protective efficacy when tested as a prophylactic vaccine in association with saponins in murine models of visceral leishmaniasis caused by *L. infantum (Dias et al., 2018; Lage et al., 2015; Martins et al., 2015; Martins et al., 2016)*. Other single analogous or chimeric constructs of the protein showed cross-protection in murine challenging with *L. amazonensis* (Martins et al., 2017)) and *L. infantum* (Dias et al., 2018). Protective immunity against leishmaniasis is proposed to be related to induction of CD4+ and CD8+ T cells, with high levels of IFN-γ and low levels of IL-10 production and a balance of IgG2a to IgG1 (Stanley and Engwerda, 2007). Adjuvants that induce a specific T helper 1 type immune response against the antigen are preferable for the development of a vaccine against leishmaniasis. Cationic liposomes, alone or in combination with immunostimulatory molecules, have been investigated to achieve safer and more effective adjuvant systems for entire or subunit antigens in vaccines against *Leishmania* and other infectious diseases. A previous study using a first generation, soluble *Leishmania* antigen (SLA) vaccine demonstrated significantly increased efficacy when the SLA was incorporated into CL with CpG and administered by the SC route (Heravi Shargh et al., 2012). We used a similar formulation to prepare vaccines against leishmaniasis containing rLiHyp1. However, in the present work, we demonstrate that these liposomes do not induce a protective immune response to *Leishmania* challenge when incorporated into DMN patches and administered into the skin.

The immunity results demonstrate that further development of the rLiHyp1 in CL is required. The aggregation of rLiHyp1, resulted from reduction of urea concentration in the protein solution, has been a major issue in the development of some vaccine systems. The influence of protein aggregation level in immunogenicity is well studied in biotherapeutics (Moussa et al., 2016; Ratanji et al., 2014). Some studies have already shown that recombinant antigen aggregates are more immunogenic and protective than monomeric or oligomeric form, when combined with adjuvants (Ahmad et al., 2017; Qian et al., 2012). It is also appreciated that particulate antigen, such as hepatitis B surface antigen

particles or HPV virus like particles are highly immunogenic. In the case of rLiHyp1, protein aggregation has two important implications regarding the mechanism of antigen delivery. First, the nanoparticulate state of the protein may contribute to differential recognition and uptake by the immune cells of mononuclear phagocytic system, as proposed previously (Herrera Estrada and Champion, 2015). This may contribute to the protective efficacy of the DMN patch incorporating the TLR9-adjuvanted antigen and the liquid vaccine containing aggregated antigen with CL and CpG. Secondly, part of the rLiHyp1 protein that is present in the CL formulation maybe self-aggregated separately from the lipid vesicles containing the antigen, as suggested by DLS, NTA and TEM images showing highly contrasted nanoparticles outside or attached to the vesicle surface. Thus, rLiHyp1 protein probably exists under three different states in the CL liposome formulation: physically encapsulated in the internal aqueous compartment of liposomes; adsorbed onto the liposome surface due to electrostatic interactions; and self-aggregated outside the liposomes. Since the encapsulation rate of liposomes was measured by centrifugation, we presume that large nanoaggregates (>150nm) of free antigen could sediment together with the liposomes and be counted as entrapped protein. In this context, the reduced concentration of protein in the centrifuged pellet after incorporation of CL into DMN could be due to a decrease of encapsulated rLiHyp1 during the DMN drying process and resuspension or to a stabilization of protein nanoaggregates in a smaller size, that remained in the supernatant during the centrifugation process. This antigen was potent when injected with CL and CpG or when incorporated with CpG in DMN patches.

Another interesting observation was that the rLiHyp1 encapsulation rate increased with the addition of CpG to the formulation. While some authors observed no influence of CpG co-encapsulation on the protein entrapment in cationic liposomes (Badiee et al., 2008), others observed the contrary, i.e. a decrease in the encapsulation efficiency when soluble proteins and CpG ODN are co-encapsulated in cationic liposomes (Bal et al., 2011). DNA-based molecules are known for inducing fusion in cationic liposomes, due to electrostatic interactions and ability to form DNA-cationic lipid complexes, such with DOTAP (Mok and Cullis, 1997). In this work, we propose that the binding of CpG ODN to the cationic membrane may have favored vesicle fusion, leading to an increase in the rLiHyp1 encapsulation into the liposomes.

DMNs containing antigen and CpG only had good mechanical robustness, however inclusion of CL weakened the DMN. The lower immunogenicity of the liposomal-DMN in comparison with rLiHyp1+CpG:DMN and the rLiHyp1+CpG:CL:SC could indicate non-optimal skin insertion for those formulations, likely related to weak DMN mechanical robustness (observed failure force of 9 N/m² compared to 17 N/m² for non-liposomal DMN), resulting in lower vaccine bioavailability. rLiHyp1-specific IgG levels produced in mice immunized by the mechanically stronger DMN, (non-liposomal, rLiHyp1+CpG), were higher compared to those generated by liposomal DMN formulations. This suggests issues in antigen and/or adjuvant bioavailability and consequently antigen recognition, uptake and presentation may be responsible for poor immunogenicity of the CL-DMN systems. A previous study, which examined transcutaneous administration of cationic liposomes charged with CpG and

ovalbumin, showed that the CL significantly decreased the antigen / CpG uptake by dendritic cells due to an extra transport step across the epidermis, although *in vitro* DC stimulation showed a higher potential of this formulation (Slutter et al., 2011). This suggests that the presence of CL in the DMN could also have impacted antigen uptake due to preferable antigen retention in the epidermis. If true, then this suggests that cationic liposomes are unsuitable as adjuvants for vaccines delivered transcutaneously. The weakness conferred by the lipids in our DMN differs from other studies. These studies suggested that very weak liposomal DMN, (bent when a force of 4N was applied) pierced the skin when applied with a force superior to 2N (Qiu et al., 2016). Other studies, did not report the DMN mechanical robustness, but have reported the capacity to induce immune responses (Guo et al., 2013). These DMN formulations are often prepared with a higher concentration of polymer (usually > 20% w/w, PVP) in comparison with 1.25% w/w of PVA contained in the formulations developed in this work. Additionally, some DMN formulations that were stated to be immunogenic (Guo et al., 2013) were fabricated based on the antigen being concentrated to the DMN tip, which may increase antigen bioavailability. Therefore, future studies should address the lack of immunogenicity with our CL DMN, possibly due to low biodistribution, by using previously described formulations and microneedle designs (Marshall et al., 2016). These results encourage, overall, the optimization and improvement of the development of CL+CpG:DMN formulations in order to increase DMN mechanical strength and vaccine bioavailability and consequently improve the protection potential of this formulation.

Skin vaccination using microneedle patches skews the antibody isotype towards a dominant IgG1, Th2-type antibody response; this has been observed across several microneedle systems (Pulit-Penaloza et al., 2014; Weldon et al., 2012). Although liposomal rLiHyp1-DMN patches induced weak humoral immune responses, when compared to non-liposomal DMN patch, the skin vaccination of mice with rLiHyp1+CpG:CL was the only one that appeared to shift the balance of IgG subtypes towards IgG2a, in some animals of this group. This fact was reinforced by a higher IFN-γ cytokine secreted by LiHyP1 stimulated splenocytes from the animals in the same group compared to all others. Unfortunately, methodological problems prevented a statistical comparison of T cell data, as a lot of splenocyte samples were not responsive to *in vitro* cytokine stimulation. Furhter studies are required to determine if the development of a CL-containing DMN patch is worthwhile with respect to modulating the immune response toward a Th1 response.

For *L. donovani* infection in the liver, the rLiHyp1+CpG:DMN vaccine induced the greatest protection among all groups, similar to subcutaneous injection of rLiHyp1+CpG:LC, whereas the liposomal DMN system was not able to induce a significant reduction in the parasite load compared to unvaccinated mice. The protective efficacy of the liposomal-based DMN may also have been compromised by the suboptimal mechanical strength of these patches and decreased antigen bioavailability. Although both the SC injected vaccine and the CpG:DMN vaccines induced significantly reduced parasite load in the spleen, only the DMN patches induced the highest reduction in parasite load also in the liver, compared to naïve animals. This indicates that skin-based vaccination, using microneedles, with the rLiHyp1 antigen and CpG adjuvant is beneficial.

15

Based on the particle size characterization of this vaccine system, it is likely that some of the LiHyp1 antigen had aggregated into a homogenous particulate suspension of acceptable PDI (Table 2). This suggests that the particulate antigen maybe beneficial to the vaccine effect. Here we suggest that adjuvanted antigen aggregates delivered into the skin are immunogenic and induce protection against parasite infection. It will be important in future studies to assess the quaternary structure of this recombinant antigen as well as the relative importance of the route and method of immunization by determining if this antigen and CpG vaccine can induce similar efficacy if it is injected.

There are significant advantages of the microneedle patch compared to injection-based immunization of liquid vaccine, with respect to the elimination of biohazardous needles, syringes and the need for cold chain, Thus, from a logistics perspective, development of a stable, easy-to-administer leishmania vaccine patch is highly desirable. Our results demonstrate that this patch-based leishmania vaccine induces highly protective immune responses. This provides a foundation for further development and optimization of this technology for eventual clinical deployment.

4   Conclusions

The results of this work prove that a skin vaccine system comprised of a rLiHyp1 associated with CpG (DMN LiHyp1 + CpG) in dissolvable microneedle patches induces excellent levels of protective immunity in mice against experimental leishmaniasis challenge. This system has a high potential for minimally invasive vaccination against leishmaniasis, presenting a promising skin-based possibility for the prevention of the disease. Secondly, this work demonstrates that dissolvable microneedle patches incorporating cationic liposomes and parasite antigens can be produced, with and without CpG. However, these patches should be further developed to improve the homogeneity of the formulation and the mechanical robustness of the microneedle. If future studies demonstrate the advantages of enhanced vaccine stability then this system presents a potential to reduce costs involved in the vaccine manufacturing, storage and application. The possibility of greater adherence by patients to an easy-to-administer vaccine format, should increase the success in vaccination programmes. In conclusion, the microneedle patch skin vaccine format proposed here represent a potential vaccine technology for the prevention of leishmaniasis that has promise for further development and translation to humans.

Declaration of Competing Interest

Sonja Vucen, Agnese Donadei and Anne Moore are inventors of patents that have been or may be licensed to companies developing microneedle-based products. This potential competing interest has been disclosed and is being managed by University College Cork. All other authors declare that they have no known competing financial interests. None of the authors have personal relationships that could have appeared to influence the work reported in this paper.

Acknowledgements

Figure Legends

Figure 1. Heterologous expression and purification of Leishmania recombinant protein LiHyp1. (A) LiHyp1 DNA sequence, cloned in plasmid, transfected in Escherichia coli and purified by FPLC. LiHyp1 3D protein model obtained using SWISS-Model Repository. (B) SDS-PAGE and (C) Western blot of the purified fractions, using anti-His tag antibody was performed to confirm purity and specificity of rLiHyp1.

Figure 2. Dissolvable microneedles patches. (A) PDMS (polydimethylsiloxane) mold for manufacturing of dissolvable microneedles (McGrath et al., 2014). (B) Macroscopic aspect of a patch (left) and an individual microneedle (right) prepared from a CL + LiHyp1 + CpG obtained through a light microscope, inverted, with a magnification of 20 times. (C) Images of rLiHyp1-liposomal DMN in lower magnitude (left) and zoomed (right) from scanning electron microscopy (SEM).

Figure 3. Size and morphology of rLiHyp1 liposomes, before and after incorporation in DMN. Size distribution (diameter, nm) of CL containing rLiHyp1 and CpG measured by NTA, (A) before or (B) after incorporation into DMN. TEM images (PTA 1% contrast agent) of CL containing rLiHyp1 (C) before and (D) after insertion in DMN; scale bar = 200nm.

Figure 4. Kinetics of DMN patch dissolution in skin. Figures represent DMN containing BSA and CpG incorporated into CL before and after application into pig skin. The time intervals evaluated were immediately after insertion or 1, 3, 5 and 15 minutes after application and maintenance. The DMN were applied with the aid of a manual applicator, calibrated with the force of 10N, perpendicular to the axial axis of the DMN.

Figure 5. Study of DMN insertion into porcine skin. (A) Scheme of DMN porcine skin application. Images of: (B) *en face* image of skin after DMN application and immediate withdrawal, with subsequent indentation staining by methylene blue stain; Bright field photomicrography of pig-skin cryosections mounted on glass slide with Entelan®. Breach made by a DMN into the skin as imaged by (C) brightfield and (D) subsequent to Trichome-Masson staining. Normal skin as imaged by (E) brightfield and (F) subsequent to Trichome-Masson staining. Magnification 400X, scale bar = 20µm. The arrow indicates where it is possible to identify a typical DMN penetration event.

Figure 6. Antibody responses induced by LiHyp1 containing vaccines. BALB/c female mice were immunized on days 0, 14 and 28 with LiHyp1 encapsulated with CpG in cationic liposomes and administered by the SC route "(LiHyp1+CpG)CL SC" or with DMN patches containing LiHyp1 and CpG encapsulated in cationic liposomes; "(LiHyp1+CpG)CL DMN", or with LiHyp1 encapsulated in cationic liposomes; "(LiHyp1)CL DMN" or with LiHyp1 and CpG incorporated into DMN patches without liposomes; "LiHyp1 +CpG DMN". Serum was assessed for LiHyp1-specific IgG (A), IgG1 (B), or IgG2a (C) on day 40. (D) Ratio of IgG2a endpoint titers to IgG1 titers in each animal. Bars represent median values with interquartile range. Symbols represent individual animals. *; $p < 0.05$; ** $p < 0.01$, significantly different to the other vaccinated groups at 8 weeks, using Kruskal-Wallis one-way ANOVA. The dotted line represents the initial serum dilution of 1/100.

Figure 7. T cell responses induced by LiHyp1 containing vaccines. IFN-γ (A) or IL-10 (B) produced by thawed spleen cells stimulated with 1µg LiHyp1 (dark bars) or with ConA (light bars) for 48 hours. BALB/c female mice were immunized as described in Figure 6. The horizontal dashed line in (B) represents the maximum background level of IL-10 produced by naïve cells stimulated with LiHyp1.

Figure 8. Protective immunity conferred by LiHyp1 vaccines in DNM patches in skin or in CL for subcutaneous injection, in a BALB/c - L. donovani murine model of visceral leishmaniasis. BALB/c mice were first immunized, as described in Figure 6 legend or a group were injected (SC) with PBS. All mice were infected with 1 x 106 L. donovani amastigotes 3 weeks after the last immunization. Parasite load was determined by qPCR absolute quantification. Statistical analysis was performed with the Kruskal-Wallis test followed by the Dunns test in relation to the PBS control, *p <0.01; **p <0.001, ***p<0,0001. The results are shown as median and interquartile range. N ≥ 7 per group.

Supplementary Figure 1. Macroscopic aspect of DMN prepared from a CL + BSA + CpG at (A) 4M of urea and (B) 0.8M of urea. The images were obtained with a light microscope, inverted, with a magnification of 20 times.

References

Ahmad, F., Zubair, S., Gupta, P., Gupta, U.D., Patel, R., Owais, M., 2017. Evaluation of Aggregated Ag85B Antigen for Its Biophysical Properties, Immunogenicity, and Vaccination Potential in a Murine Model of Tuberculosis Infection. Front Immunol 8, 1608.

Badiee, A., Jaafari, M.R., Samiei, A., Soroush, D., Khamesipour, A., 2008. Coencapsulation of CpG oligodeoxynucleotides with recombinant Leishmania major stress-inducible protein 1 in liposome enhances immune response and protection against leishmaniasis in immunized BALB/c mice. Clin Vaccine Immunol 15, 668-674.

Bal, S.M., Slutter, B., Jiskoot, W., Bouwstra, J.A., 2011. Small is beautiful: N-trimethyl chitosan-ovalbumin conjugates for microneedle-based transcutaneous immunisation. Vaccine 29, 4025-4032.

Balaraman, K., Vieira, N.C., Moussa, F., Vacus, J., Cojean, S., Pomel, S., Bories, C., Figadere, B., Kesavan, V., Loiseau, P.M., 2015. In vitro and in vivo antileishmanial properties of a 2-n-propylquinoline hydroxypropyl beta-cyclodextrin formulation and pharmacokinetics via intravenous route. Biomed Pharmacother 76, 127-133.

Bhowmick, S., Ravindran, R., Ali, N., 2008. gp63 in stable cationic liposomes confers sustained vaccine immunity to susceptible BALB/c mice infected with Leishmania donovani. Infect Immun 76, 1003-1015.

Christensen, D., Korsholm, K.S., Andersen, P., Agger, E.M., 2011. Cationic liposomes as vaccine adjuvants. Expert Rev Vaccines 10, 513-521.

Coelho, V.T., Oliveira, J.S., Valadares, D.G., Chavez-Fumagalli, M.A., Duarte, M.C., Lage, P.S., Soto, M., Santoro, M.M., Tavares, C.A., Fernandes, A.P., Coelho, E.A., 2012. Identification of proteins in promastigote and amastigote-like Leishmania using an immunoproteomic approach. PLoS Negl Trop Dis 6, e1430.

De Serrano, L.O., Burkhart, D.J., 2017. Liposomal vaccine formulations as prophylactic agents: design considerations for modern vaccines. J Nanobiotechnology 15, 83.

Dias, D.S., Ribeiro, P.A.F., Martins, V.T., Lage, D.P., Costa, L.E., Chavez-Fumagalli, M.A., Ramos, F.F., Santos, T.T.O., Ludolf, F., Oliveira, J.S., Mendes, T.A.O., Silva, E.S., Galdino, A.S., Duarte, M.C., Roatt, B.M., Menezes-Souza, D., Teixeira, A.L., Coelho, E.A.F., 2018. Vaccination with a CD4(+) and CD8(+) T-cell epitopes-based recombinant chimeric protein derived from Leishmania infantum proteins confers protective immunity against visceral leishmaniasis. Transl Res 200, 18-34.

Donadei, A., Kraan, H., Ophorst, O., Flynn, O., O'Mahony, C., Soema, P.C., Moore, A.C., 2019. Skin delivery of trivalent Sabin inactivated poliovirus vaccine using dissolvable microneedle patches induces neutralizing antibodies. J Control Release 311-312, 96-103.

Duarte, M.C., Lage, D.P., Martins, V.T., Chavez-Fumagalli, M.A., Roatt, B.M., Menezes-Souza, D., Goulart, L.R., Soto, M., Tavares, C.A., Coelho, E.A., 2016. Recent updates and perspectives on approaches for the development of vaccines against visceral leishmaniasis. Rev Soc Bras Med Trop 49, 398-407.

Duttagupta, C., Bhattacharyya, D., Narayanan, P., Pattanshetty, S.M., 2017. Vaccine wastage at the level of service delivery: a cross-sectional study. Public Health 148, 63-65.

Fehres, C.M., Garcia-Vallejo, J.J., Unger, W.W., van Kooyk, Y., 2013. Skin-resident antigen-presenting cells: instruction manual for vaccine development. Front Immunol 4, 157.

Fernandes, A.P., Coelho, E.A., Machado-Coelho, G.L., Grimaldi, G., Jr., Gazzinelli, R.T., 2012. Making an anti-amastigote vaccine for visceral leishmaniasis: rational, update and perspectives. Curr Opin Microbiol 15, 476-485.

Fernandez Cotrina, J., Iniesta, V., Monroy, I., Baz, V., Hugnet, C., Maranon, F., Fabra, M., Gomez-Nieto, L.C., Alonso, C., 2018. A large-scale field randomized trial demonstrates safety and efficacy of the vaccine LetiFend(R) against canine leishmaniosis. Vaccine 36, 1972-1982.

Filipe, V., Hawe, A., Jiskoot, W., 2010. Critical evaluation of Nanoparticle Tracking Analysis (NTA) by NanoSight for the measurement of nanoparticles and protein aggregates. Pharm Res 27, 796-810.

Frezard, F., 1999. Liposomes: from biophysics to the design of peptide vaccines. Braz J Med Biol Res 32, 181-189.

Gillespie, P.M., Beaumier, C.M., Strych, U., Hayward, T., Hotez, P.J., Bottazzi, M.E., 2016. Status of vaccine research and development of vaccines for leishmaniasis. Vaccine 34, 2992-2995.

Guo, L., Chen, J., Qiu, Y., Zhang, S., Xu, B., Gao, Y., 2013. Enhanced transcutaneous immunization via dissolving microneedle array loaded with liposome encapsulated antigen and adjuvant. Int J Pharm 447, 22-30.

Heravi Shargh, V., Jaafari, M.R., Khamesipour, A., Jalali, S.A., Firouzmand, H., Abbasi, A., Badiee, A., 2012. Cationic liposomes containing soluble Leishmania antigens (SLA) plus CpG ODNs induce protection against murine model of leishmaniasis. Parasitol Res 111, 105-114.

Herrera Estrada, L.P., Champion, J.A., 2015. Protein nanoparticles for therapeutic protein delivery. Biomater Sci 3, 787-799.

Joyce, C., Scallan, C.D., Mateo, R., Belshe, R.B., Tucker, S.N., Moore, A.C., 2018. Orally administered adenoviral-based vaccine induces respiratory mucosal memory and protection against RSV infection in cotton rats. Vaccine 36, 4265-4277.

Kristensen, D.D., Lorenson, T., Bartholomew, K., Villadiego, S., 2016. Can thermostable vaccines help address cold-chain challenges? Results from stakeholder interviews in six low- and middle-income countries. Vaccine 34, 899-904.

Lage, D.P., Martins, V.T., Duarte, M.C., Garde, E., Chavez-Fumagalli, M.A., Menezes-Souza, D., Roatt, B.M., Tavares, C.A., Soto, M., Coelho, E.A., 2015. Prophylactic properties of a Leishmania-specific hypothetical protein in a murine model of visceral leishmaniasis. Parasite Immunol 37, 646-656.

Li, M., Du, C., Guo, N., Teng, Y., Meng, X., Sun, H., Li, S., Yu, P., Galons, H., 2019. Composition design and medical application of liposomes. Eur J Med Chem 164, 640-653.

Manna, L., Reale, S., Vitale, F., Picillo, E., Pavone, L.M., Gravino, A.E., 2008. Real-time PCR assay in Leishmania-infected dogs treated with meglumine antimoniate and allopurinol. Vet J 177, 279-282.

Marfurt, J., Nasereddin, A., Niederwieser, I., Jaffe, C.L., Beck, H.P., Felger, I., 2003. Identification and differentiation of Leishmania species in clinical samples by PCR amplification of the miniexon sequence and subsequent restriction fragment length polymorphism analysis. J Clin Microbiol 41, 3147-3153.

Marshall, S., Sahm, L.J., Moore, A.C., 2016. The success of microneedle-mediated vaccine delivery into skin. Hum Vaccin Immunother 12, 2975-2983.

Martin, V., Vouldoukis, I., Moreno, J., McGahie, D., Gueguen, S., Cuisinier, A.M., 2014. The protective immune response produced in dogs after primary vaccination with the LiESP/QA-21 vaccine (CaniLeish(R)) remains effective against an experimental challenge one year later. Vet Res 45, 69.

Martins, V.T., Chavez-Fumagalli, M.A., Costa, L.E., Canavaci, A.M., Martins, A.M., Lage, P.S., Lage, D.P., Duarte, M.C., Valadares, D.G., Magalhaes, R.D., Ribeiro, T.G., Nagem, R.A., Darocha, W.D., Regis, W.C., Soto, M., Coelho, E.A., Fernandes, A.P., Tavares, C.A., 2013. Antigenicity and protective efficacy of a Leishmania amastigote-specific protein, member of the super-oxygenase family, against visceral leishmaniasis. PLoS Negl Trop Dis 7, e2148.

Martins, V.T., Chavez-Fumagalli, M.A., Lage, D.P., Duarte, M.C., Garde, E., Costa, L.E., da Silva, V.G., Oliveira, J.S., Magalhaes-Soares, D.F., Teixeira, S.M., Fernandes, A.P., Soto, M., Tavares, C.A., Coelho, E.A., 2015. Antigenicity, Immunogenicity and Protective Efficacy of Three Proteins Expressed in the Promastigote and Amastigote Stages of Leishmania infantum against Visceral Leishmaniasis. PLoS One 10, e0137683.

Martins, V.T., Lage, D.P., Duarte, M.C., Carvalho, A.M., Costa, L.E., Mendes, T.A., Vale, D.L., Menezes-Souza, D., Roatt, B.M., Tavares, C.A., Soto, M., Coelho, E.A., 2017. A recombinant fusion protein displaying murine and human MHC class I- and II-specific epitopes protects against Leishmania amazonensis infection. Cell Immunol 313, 32-42.

Martins, V.T., Lage, D.P., Duarte, M.C., Costa, L.E., Garde, E., Rodrigues, M.R., Chavez-Fumagalli, M.A., Menezes-Souza, D., Roatt, B.M., Tavares, C.A., Soto, M., Coelho, E.A., 2016. A new Leishmania-specific hypothetical protein, LiHyT, used as a vaccine antigen against visceral leishmaniasis. Acta Trop 154, 73-81.

McGrath, M.G., Vucen, S., Vrdoljak, A., Kelly, A., O'Mahony, C., Crean, A.M., Moore, A., 2014. Production of dissolvable microneedles using an atomised spray process: effect of microneedle composition on skin penetration. Eur J Pharm Biopharm 86, 200-211.

Mok, K.W., Cullis, P.R., 1997. Structural and fusogenic properties of cationic liposomes in the presence of plasmid DNA. Biophys J 73, 2534-2545.

Moussa, E.M., Panchal, J.P., Moorthy, B.S., Blum, J.S., Joubert, M.K., Narhi, L.O., Topp, E.M., 2016. Immunogenicity of Therapeutic Protein Aggregates. J Pharm Sci 105, 417-430.

Nayar, R., Hope, M.J., Cullis, P.R., 1989. Generation of large unilamellar vesicles from long-chain saturated phosphatidylcholines by extrusion technique. Biochimica et Biophysica Acta (BBA) - Biomembranes 986, 200-206.

Nicolas, L., Prina, E., Lang, T., Milon, G., 2002. Real-time PCR for detection and quantitation of leishmania in mouse tissues. J Clin Microbiol 40, 1666-1669.

Noazin, S., Modabber, F., Khamesipour, A., Smith, P.G., Moulton, L.H., Nasseri, K., Sharifi, I., Khalil, E.A., Bernal, I.D., Antunes, C.M., Kieny, M.P., Tanner, M., 2008. First generation leishmaniasis vaccines: a review of field efficacy trials. Vaccine 26, 6759-6767.

O'Mahony, C., 2014. Structural characterization and in-vivo reliability evaluation of silicon microneedles. Biomed Microdevices 16, 333-343.

Paleco, R., Vucen, S.R., Crean, A.M., Moore, A., Scalia, S., 2014. Enhancement of the in vitro penetration of quercetin through pig skin by combined microneedles and lipid microparticles. Int J Pharm 472, 206-213.

Peterson, G.L., 1977. A simplification of the protein assay method of Lowry et al. which is more generally applicable. Anal Biochem 83, 346-356.

Pulit-Penaloza, J.A., Esser, E.S., Vassilieva, E.V., Lee, J.W., Taherbhai, M.T., Pollack, B.P., Prausnitz, M.R., Compans, R.W., Skountzou, I., 2014. A protective role of murine langerin(+) cells in immune responses to cutaneous vaccination with microneedle patches. Sci Rep 4, 6094.

Qian, F., Reiter, K., Zhang, Y., Shimp, R.L., Jr., Nguyen, V., Aebig, J.A., Rausch, K.M., Zhu, D., Lambert, L., Mullen, G.E., Martin, L.B., Long, C.A., Miller, L.H., Narum, D.L., 2012. Immunogenicity of self-associated aggregates and chemically cross-linked conjugates of the 42 kDa Plasmodium falciparum merozoite surface protein-1. PLoS One 7, e36996.

Qiu, Y., Guo, L., Zhang, S., Xu, B., Gao, Y., Hu, Y., Hou, J., Bai, B., Shen, H., Mao, P., 2016. DNA-based vaccination against hepatitis B virus using dissolving microneedle arrays adjuvanted by cationic liposomes and CpG ODN. Drug Deliv 23, 2391-2398.

Ratanji, K.D., Derrick, J.P., Dearman, R.J., Kimber, I., 2014. Immunogenicity of therapeutic proteins: influence of aggregation. J Immunotoxicol 11, 99-109.

Santi, A.M.M., Lanza, J.S., Tunes, L.G., Fiuza, J.A., Roy, G., Orfano, A.D.S., de Carvalho, A.T., Frezard, F., Barros, A.L.B., Murta, S.M.F., do Monte-Neto, R.L., 2018. Growth arrested live-attenuated Leishmania infantum KHARON1 null mutants display cytokinesis defect and protective immunity in mice. Sci Rep 8, 11627.

Schwendener, R.A., 2014. Liposomes as vaccine delivery systems: a review of the recent advances. Ther Adv Vaccines 2, 159-182.

Slutter, B., Bal, S.M., Ding, Z., Jiskoot, W., Bouwstra, J.A., 2011. Adjuvant effect of cationic liposomes and CpG depends on administration route. J Control Release 154, 123-130.

Stanley, A.C., Engwerda, C.R., 2007. Balancing immunity and pathology in visceral leishmaniasis. Immunol Cell Biol 85, 138-147.

Toepp, A., Larson, M., Wilson, G., Grinnage-Pulley, T., Bennett, C., Leal-Lima, A., Anderson, B., Parrish, M., Anderson, M., Fowler, H., Hinman, J., Kontowicz, E., Jefferies, J., Beeman, M., Buch, J., Saucier, J., Tyrrell, P., Gharpure, R., Cotter, C., Petersen, C., 2018. Randomized, controlled, double-blinded field trial to assess Leishmania vaccine effectiveness as immunotherapy for canine leishmaniosis. Vaccine 36, 6433-6441.

Uliana, S.R.B., Trinconi, C.T., Coelho, A.C., 2018. Chemotherapy of leishmaniasis: present challenges. Parasitology 145, 464-480.

Vrdoljak, A., Allen, E.A., Ferrara, F., Temperton, N.J., Crean, A.M., Moore, A.C., 2016. Induction of broad immunity by thermostabilised vaccines incorporated in dissolvable microneedles using novel fabrication methods. J Control Release 225, 192-204.

Vucen, S.R., Vuleta, G., Crean, A.M., Moore, A.C., Ignjatovic, N., Uskokovic, D., 2013. Improved percutaneous delivery of ketoprofen using combined application of nanocarriers and silicon microneedles. J Pharm Pharmacol 65, 1451-1462.

Weldon, W.C., Zarnitsyn, V.G., Esser, E.S., Taherbhai, M.T., Koutsonanos, D.G., Vassilieva, E.V., Skountzou, I., Prausnitz, M.R., Compans, R.W., 2012. Effect of adjuvants on responses to skin immunization by microneedles coated with influenza subunit vaccine. PLoS One 7, e41501.

Zadi, B., Gregoriadis, G., 2000. A Novel Method for High-Yield Entrapment of Solutes into Small Liposomes. Journal of Liposome Research 10, 73-80.
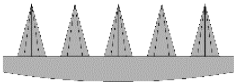
Table 1. DMN 4-tier scoring system

Score	DMN Description	Scheme
4	'Perfect DMN': 8 sided DMN, sharp tips	
3	'Near Perfect DMN': 6-4 sided DMN or cone shaped or wizard hat or blunt tip	
2	'Volcano type', no tip	
1	Stub/no DMN	

Table 2- Biophysical characteristics of LiHyp1 formulations

Format	Sample	Mean size (d.nm) ± SD	PDI ± SD	Zeta P. (mV) ± SD	ER %	Pressure required for DMN failure (N/m^2)	DMN Score
Soluble	LiHyp1 in PBS 8M urea	70.0 ± 8.3	0.20 ± 0.02	-12.0 ± 0.1	NA	NA	NA
	[1]LiHyp1 in PBS 4M urea	198.5 ± 7.6	0.37 ± 0.01	-14.2 ± 0.3	NA	NA	NA
	[2]LiHyp1 0.8M urea in Trehalose 15% (w/v) + PVA 1.25% (w/v)	158.4± 9.7	0.17± 0.01	-10.1±1.2	N/A	N/A	N/A
[3]Liposome encapsulated	LiHyp1 in CL	218.3 ±31.8	0.60± 0.25	+23.3± 0.7	41±12	N/A	N/A
	LiHyp1 + CpG in CL	186.2 ± 43.2	0.57± 0.09	+20.0± 0.4	77±23	N/A	N/A
[4]Solid	DMN LiHyp1 in CL	237.5 ±15.4	0.89± 0.42	+26.6± 0.8	24±9	10.2	95
	DMN LiHyp1 + CpG in CL	239.5 ±23.4	0.70± 0.41	+20.3± 1.4	49±6	9.5	96
	DMN LiHyp1 + CpG	176.5 ±22.6	0.13± 0.06	-13.5±0.6	NA	17.4	98

[1]LiHyp1 in PBS solution containing 4 M urea was prepared by dialysis of the initial purified LiHyp1 in PBS/8 M urea. [2]LiHyp1 initial purified solution was dialyzed into the DMN formulation, trehalose 15% (w/v) + PVA 1.25% (w/v) containing 0.8M of urea, in order to equilibrate the solutes' concentration. [3]Liposome-encapsulated samples were diluted (100x) in PBS (size) or water (zeta potential) before DLS and NTA measurements. [4]Each DMN patch was dissolved in 1 mL of PBS before NTA and DLS measurements. CL: cationic liposome; Mean size (d.nm): average of results of particle size measurements by NTA technique. SD: standard deviation. PDI: polydispersity index given by DLS technique. Zeta P.: Zeta potential in millivolts (mV), measured by DLS. ER: Encapsulation rate in percentage. Pressure is given in Newtons per square meter (N/m^2); The DMN were scored based on DMN '4-tier' scoring system – Table 1

Juliane S. Lanza; Conceptualization, Data curation; Formal analysis; Funding acquisition; Investigation; Methodology Writing - original draft preparation, reviewing and editing

Sonja Vucen; Supervision, Formal analysis, Investigation; Methodology, Project administration,Resources, Writing - review & editing

Olivia Flynn; Supervision, Methodology Formal analysis, Investigation, Validation Data curation,

Agnese Donadei; Supervision, Methodology, Formal analysis, Validation, Investigation

Sandrine Cojean; Supervision, Investigation, Methodology Resources

Philippe Loiseau; Supervision, Investigation, Methodology, Resources

Ana Paula S. M. Fernandes; Supervision, Investigation, Methodology, Resources

Frédéric Frézard; Conceptualization, Funding acquisition, Supervision, Methodology, Resources, Writing - review & editing

Anne C. Moore; Conceptualization, Data curation; Formal analysis; Funding acquisition; Investigation; Methodology; Project administration; Resources;; Supervision; Validation; Visualization; Roles/Writing - original draft; Writing - review & editing

Graphical Abstract

rLHyp1 / CpG associated CL

CpG
ODN

Cationic liposome (CL)

Soluble rLiHyp1
or its aggregates

DMN skin application

DMN dissolution and liberation of content

Epidermis

Dermis

Mice protected against leishmaniasis